IET Generation, Transmission & Distribution

Research Article

IET Journals
The Institution of Engineering and Technology

Synchro-phasors Assisted Back-up Protection of Transmission Line

ISSN 1751-8687
Received on 1st November 2017
Accepted on 24th April 2018
E-First on 31st May 2018
doi: 10.1049/iet-gtd.2017.1711
www.ietdl.org

Vibhuti Nougain[1] ✉, *Manas K. Jena*[2], *Bijaya K. Panigrahi*[1]

[1]*Electrical Engineering Department, Indian Institute of Technology, Delhi, India*
[2]*General Electric (GE Power) HTC, India*
✉ *E-mail: vibhutinougain91@gmail.com*

Abstract: Certain power system situations force protection schemes to mal-operate. Such mal-operations associated with back-up protection (BP) schemes might worsen the situation by initiating the cascading effect, damaging critical elements such as generation units, transformers etc. of the power system, or leading to complete collapse of the power system. To adapt to such a network structure, the relays which are going to participate in BP of transmission line have to evolve. Integration of protection systems, communication network, and computer technology has to be the approach for faster information sharing and decision making. Analysis of recent blackouts clearly shows the importance of advancement of wide-area measurement systems and adaptive nature of relaying. Synchro-phasors assisted BP scheme is proposed in this work, which helps the relays adapt according to the prevailing system situations and decisive action is taken considering security and dependability aspects of the relays.

1 Introduction

Inadequate operation of protection principles governing the protection schemes associated with various power system elements have caused severe wide-area disturbances and blackouts in recent past [1–5]. Such incidents raise questions on the reliability of the existing protection schemes. The huge complexity of the current national grids across the globe demands for more dependable and secure protection of the power network. The main culprit of such failures has been the mal-operation of the distance relays which are meant to identify faults on the protected transmission line and beyond [3]. Distance relays are installed to have both primary as well as back-up protection (BP), and it is the BP which causes line tripping after seeing power swings or load encroachment conditions as faults [1–3]. For the generation of trip signal, apparent impedance should stay within the ʊ circle for a time interval which is greater than the intentional time delay associated with the zone-3 relay [4]. This triggers opening of the corresponding circuit breakers, leading to unnecessary line outages in the system. Other lines in the system get overloaded and further tripping initiates the cascading effect leading to huge disturbances and generators going out of synchronisation one after the other, causing complete blackout. The most significant point to be studied in this scenario is that the triggering event is a no fault situation. Thus, differentiating fault situations from other power system disturbances which behave like fault condition, is vital for reliable operation of power system. Proper communication and supervision of the power system and evolution of BP schemes are the need of the hour [6–9]. Third zone unwanted tripping caused by unexpected loading conditions has been observed and often contributed to the cascaded outages, and eventually leading to major blackouts [10–15].

In [10], the above-mentioned problem is revisited by the authors and in [11]; the literature concludes that zone-3 protection logic must be made immune to false tripping under heavy loading conditions. In [12], a new adaptive load encroachment prevention scheme is suggested by Jin and Sidhu. It is based on the identification of 'hidden failures' from steady-state security analysis to prevent false tripping due to excessive loading. However, power swing also leads to zone-3 mal-operation, and thus its impact on protection schemes should be arrested for the proper functioning of the protection logic. In [13], a protection scheme is presented which depends on observing positive-sequence voltage magnitudes for specified areas and phase difference angles of positive-sequence current for each interconnected line between two areas on the network to identify the faults on the transmission lines. Dependability–security aspects of the relay for transmission lines are discussed in [14, 15]. BP scheme for the series compensated line is discussed in [16]. In this domain itself, another contribution was done by Zare *et al.* in [17]. In this, the proposed methodology operates on positive-sequence synchro-phasor data captured by PMUs dispersed over the network or digital relays with synchronisation capability. The basic concept is to compare the bus voltage values calculated through dissimilar paths. In [18], a new feature termed as 'phase angle of positive-sequence integrated impedance' is introduced to locate the faulted line in a wide-area network. In the same line of thought, in [19], a Koopman analysis-based WABP scheme is developed to identify the faulted line in a power transmission network. However, the performance of the scheme during contingencies is not verified. In [20], a decentralised approach-based WABP scheme is suggested. Here, a new index termed as 'gain in momentum' is introduced to locate vulnerable protection zone (VPZ). Thereafter, the faulted line is identified using reactive power information of lines within the VPZ. In the aforementioned literatures, the basic protection idea is to replace the existing conventional zone-3 BP (CZBP) schemes with their proposed schemes. However, the presented work aims to assist/supervise the existing CZBP scheme based on prevailing system conditions. 'The worst situation of the proposed scheme does not deteriorate the performance of the prevailing protection scheme, and thus provides a 'win–win' situation to the existing protection logic'. The concurrent work proposes synchro-phasors assisted BP (SABP) scheme, which maintains the balance between dependability–security aspects of the distance relay based on system state, thus, preventing mal-operation of these relays that may, otherwise, have the potential to mal-operate due to certain system conditions.

The remainder of this paper is organised as follows. Section 2 discusses the proposed methodology. Section 3 presents the simulation results and results analysis. Section 4 concludes this piece of work.

2 Proposed methodology

This section primarily discusses the proposed SABP scheme. There is a sequence of events which take place to develop the new

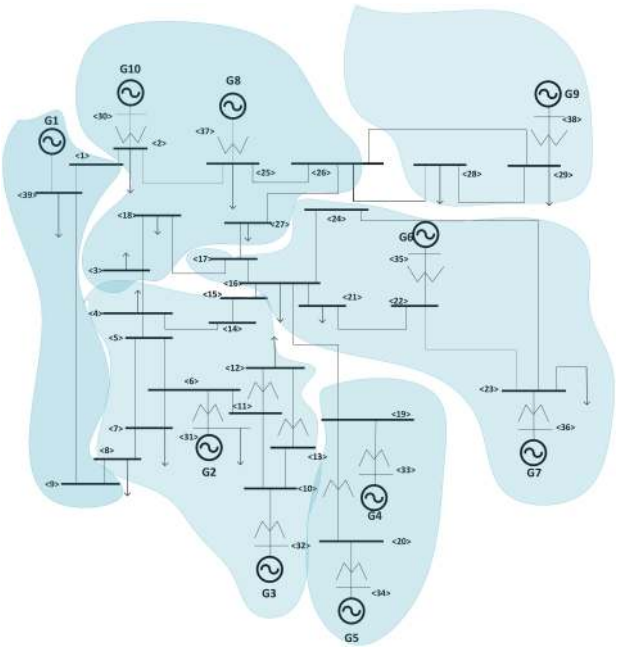

Fig. 1 *Test system – IEEE 39-bus New England power system*

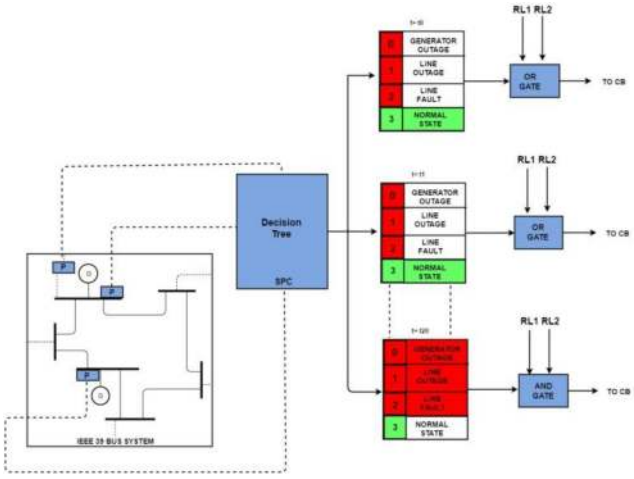

Fig. 2 *Framework of proposed methodology*

approach of adaptive relaying. The performance of SABP scheme is validated on IEEE 39-bus New England Power System shown in Fig. 1.

The SABP scheme requires PMU information at SPC. The collected phasor information is processed and the selected system variables, also called as features, participate to declare the system state using a predictive data-mining tool termed as decision tree (DT). It is important to assess the state of the system. Depending on the system state, the relay logics (RLs) interact to maintain dependability–security bias. After the declaration of the health/state of the system by DT, a warning signal is sent from SPC and the RLs, RL-1 and RL-2 switch the logic gates accordingly. It is only during stressed system state when RL-1 has the tendency to lose dependability, RL-2 comes into the picture to assist RL-1. Thus, the overall dependability of the BP logic is not disturbed during normal system condition. The overall framework is illustrated in Fig. 2.

The sequence in which various algorithms are executed to obtain a reliable relaying decision is detailed below.

2.1 Data mining

In this piece of work, an offline study is done and the test system is subjected to various ($N-1$) contingencies as well as maintenance outages such as:

- Generator outage.
- Line outage.
- Three-phase fault with different fault resistances.

Newton–Raphson load flow is made to run and the load flow data is recorded to train and test DT tool. Positive-sequence voltage magnitude, voltage angle, and delta difference of the connected buses are taken to decide the features to be fed to DT. The total number of features considered for the IEEE 39-bus test system is 112 against the target output, which tells the event/contingency. The target output is classified as 0, 1, 2, and 3 corresponding to generator outage, line outage, line fault, and normal state of the system, respectively. Out of the four mentioned target outputs, the first three (0, 1, 2) correspond to **'**STRESSED**'** system condition, while the last output (3) corresponds to **'**NORMAL**'** system condition.

In the proposed scheme, total number of features considered = 112, $|\Delta V_i|^2$ of 39 buses = 39, $|\Delta\delta_i|$ of 39 buses = 39, and $|\Delta\delta_{ij})|$ between connected buses A and B, 46 lines = 34 (46–12 transformer connections), where $|\Delta V_i|^2$ is the difference between positive-sequence voltage magnitude at the ith bus after the contingency and the positive-sequence voltage magnitude at the same bus in normal system condition, $|\Delta\delta_i|$ is the difference between positive-sequence voltage angle at the ith bus after the contingency and the positive-sequence voltage angle at the same bus in normal system condition, $|\delta_{ij}|$ is the magnitude of the angular difference between connected buses i and j, $|\Delta\delta_{ij}|$ is the magnitude of the difference between δ_{ij} after the contingency and under normal system condition.

2.2 Reduction of number of PMUs

To develop the input matrix of DT, there has to be a trade-off between the time taken to obtain the classification (0, 1, 2, and 3) and a number of features (accuracy). Thus, the redundant features are removed and model reduction is adopted to reduce the computation time by DT. In this paper, the test system is divided into six strongly coupled areas [21–23] and $|\Delta\delta_{ij}|$ as a feature is included corresponding only to the boundary buses such as (1, 2), (3, 4), (8, 9), (15, 16), (16, 19), (27, 17), (26, 28), and (26, 29). Furthermore, PMUs have to be strategically located without compromising the system information. Following 'correlation' and 'variable importance analysis', it has been observed that critical locations in the given test system are generator buses and boundary buses. There are ten generator buses in the system as shown in Fig. 1. Also, there are eight inter-area periphery locations within which the PMUs are installed on the boundary buses. Considering these strategic locations, it has been observed that out of 112 possible features, only 28 features are selected to be taken into account. The remaining system features are seen to be redundant and their inclusion would only increase decision time of DT without affecting the accuracy.

2.3 Event identification

The optimal numbers of 28 features which are dominant in classifying the target output efficiently in the DT algorithm, and thus are used in DT for building the intelligent and adaptive relay are as follows:

$$X_1 = |\Delta V|^2_{39},\ X_2 = |\Delta V|^2_{31},\ X_3 = |\Delta V|^2_{32},\ X_4 = |\Delta V|^2_{33},$$

$$X_1 = |\Delta V|^2_{39},\ X_2 = |\Delta V|^2_{31},\ X_3 = |\Delta V|^2_{32},\ X_4 = |\Delta V|^2_{33},$$

$$X_5 = |\Delta V|^2_{34},\ X_6 = |\Delta V|^2_{35},\ X_7 = |\Delta V|^2_{36},\ X_8 = |\Delta V|^2_{37},$$

$$X_9 = |\Delta V|^2_{38},\ X_{10} = |\Delta V|^2_{30},\ X_{70} = |\Delta\delta|_{30},\ X_{71} = |\Delta\delta|_{31},$$

$$X_{72} = |\Delta\delta|_{32},\ X_{73} = |\Delta\delta|_{33},\ X_{74} = |\Delta\delta|_{34},\ X_{75} = |\Delta\delta|_{35},$$

$$X_{78} = |\Delta\delta|_{36},\ X_{79} = |\Delta\delta|_{37},\ X_{80} = |\Delta\delta|_{38},\ X_{81} = |\Delta\delta|_{39},$$

$$X_{35} = |\Delta\delta|_{1,\,2},\ X_{39} = |\Delta\delta|_{3,\,4},\ X_{48} = |\Delta\delta|_{8,\,9},\ X_{55} = |\Delta\delta|_{15,\,16},$$

$$X_{58} = |\Delta\delta|_{16,\,19},\ X_{61} = |\Delta\delta|_{27,\,17},\ X_{66} = |\Delta\delta|_{26,\,28},\ X_{68} = |\Delta\delta|_{26,\,29}$$

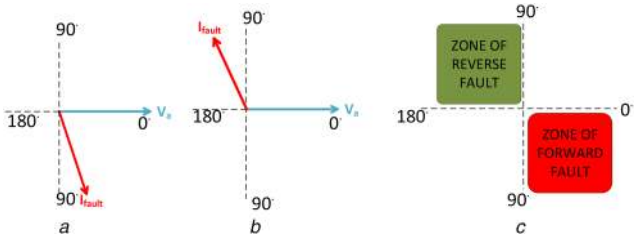

Fig. 3 *Relay logic-2: DOAPF*

(a) Phasor representation of voltage and current phasors in forward fault, ***(b)*** Phasor representation of voltage and current phasors in reverse fault, ***(c)*** Zone of forward fault and reverse fault

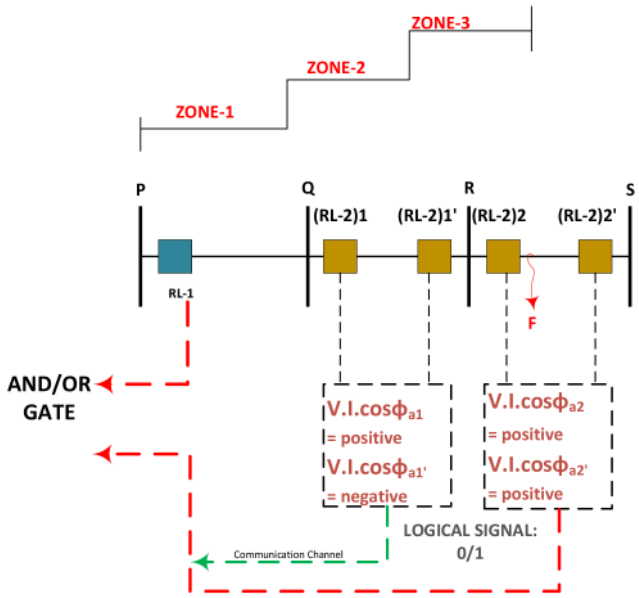

Fig. 4 *RL-2 algorithm based on DOAPF*

The event identification (EI) in the test system is realised by following the steps given below:

Step 1: *Preparation of dataset*: Various operating points of the test system are simulated to prepare a huge dataset.
Step 2: Data processing: dataset is processed and required calculations are done to obtain the values of 28 features, which are finally participating in EI.
Step 3: *Train: validate: test*: In this piece of work, it has been found that at 70:0:30 combination of dataset, the DT starts providing 100% accuracy.
Step 4: *EI*: After proper training and validation of the datasets, the optimal DT is selected which identifies the system state. DT concludes whether the system is NORMAL or STRESSED (generator outage, line outage, and line fault). This decision is communicated to the two RLs, which interact differently depending on the system state defined by DT decision.

2.4 Relay logic-2: direction of active power flow

The proposed RL-2 is synchro-phasor measurement-based RL which is employed to interact with RL-1. It is based on the concept of identification of 'forward fault' and 'reverse fault' from relay point of view [24, 25]. The proposed RL utilises the directionality property of a relay. Distance relay functions differently for 'forward fault' and 'reverse fault' [24, 25]. Detection of 'forward fault' can be done if the cosine of the angle between the measured voltage and current phasors maintain the positive value at both the ends of the transmission line. This can be understood by looking at the phasor diagram given in Fig. 3.

Mathematically, '*forward fault*' can be expressed as

$$\cos(\varnothing_v - \varnothing_i) > 0 \tag{1}$$

This is possible only if $\varnothing_v - \varnothing_i$ lies between −90° and +90°. $\varnothing_v$ and $\varnothing_i$ are the angles corresponding to voltage and current phasors. According to the suggested logic (RL-2), the zone of '*forward fault*' lies in the fourth quadrant, i.e. 0° to −90°.

Similarly, '*reverse fault*' can be expressed as

$$\cos(\varnothing_v - \varnothing_i) < 0 \tag{2}$$

Thus, the zone of '*reverse fault*' has to lie between +90° and +270°. The suggested algorithm of RL-2 obtains the zone of '*reverse fault*' in the second quadrant, i.e. +90° to +180°. However, if the *root-mean-square* values of voltage and current are multiplied by $\cos(\varnothing_v - \varnothing_i)$ of (1), the resulting expression is still able to validate the occurrence of '*forward fault*'. The resulting expression is given as

$$|V_{\text{rms}}||I_{\text{rms}}|\cos(\varnothing_v - \varnothing_i) \tag{3}$$

The above expression is termed as direction of active power flow (DOAPF), which becomes positive for '*forward fault*' and negative for '*reverse fault*'.

In the existing SCADA/EMS-based smart grid infrastructure, the active power flow information usually comes to load dispatch centres. Thus, it is possible to detect a 'forward fault' using the direction of real power information from both ends of the transmission line.

If an internal fault is incepted on line R–S as shown in Fig. 4, DOAPF for both $(\text{RL-2})_2$ and $(\text{RL-2})_{2'}$ is positive. However, for $(\text{RL2})_{1'}$, the fault *F* is a reverse fault. Thus, DOAPF for $(\text{RL-2})_{1'}$ is negative. This very concept of DOAPF is utilised in the proposed scheme in assisting the existing CZBP scheme in taking a secure relaying decision. Furthermore, it is also observed that DOAPF-based RL is reliable even during stressed conditions such as load encroachment and power swing.

3 Test cases and result analysis

The proposed algorithm is tested for normal operating conditions as well as under various stressed system circumstances such as faults, stable power swing, load encroachment, $(N-1)$ contingencies etc. on 39-bus New England Power System using MATLAB/SIMULINK platform. The impact of various latencies associated with wide-area measurement system-based infrastructure on the performance of the proposed SABP scheme is also discussed in this section. Extensive simulation results are detailed in the following sections.

3.1 Performance of DT

The state assessment is accomplished by training the DT, which is the employed data-mining tool in this work. The dataset is generated by simulating various disturbances such as generator outage (7 numbers), line outage (34 numbers), and line faults with variations in fault parameters. To the above dataset, white Gaussian noise with a signal-to-noise ratio of 20 dB is added to test the performance of the predictive model during noisy condition. Fig. 5 shows the optimal DT obtained after training process and the nodes of the tree represent features, which are participating in classifying the events.

The confusion matrix is shown in Table 1. Out of the total set of data of more than 4000 operating points of the test system; only 393 cases are considered as test cases to test the accuracy of DT. After observing the confusion matrix, it has been found that there is one misclassification of the event which is misclassified as three-phase line fault. However, this misclassification does not deteriorate the performance of the EI algorithm because the final DT output still declares the misclassified state as 'STRESSED'. Table 2 shows error matrix corresponding to the confusion matrix.

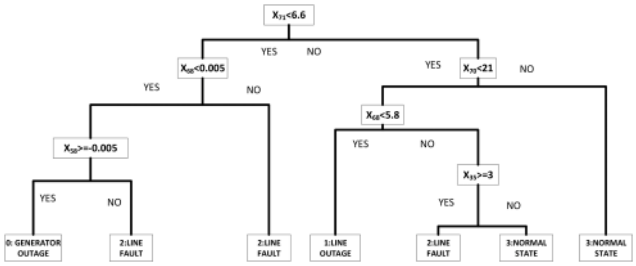

Fig. 5 *Optimal DT and important features participating in EI*

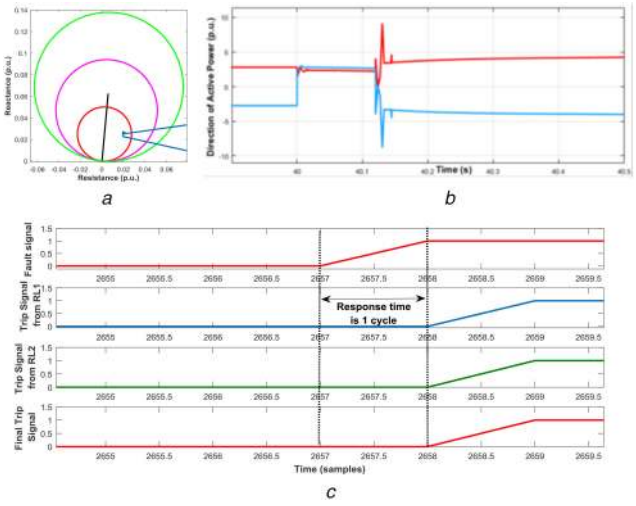

Fig. 6 *Performance of SABP scheme under 'NORMAL' system state*
(a) Trajectory of apparent impedance of the relay under three-phase fault on line 26–29, ***(b)*** DOAPF of RL-2 corresponding to line 26–29 under three-phase fault on line 26–29, ***(c)*** Trip signals generated from RL-1 and RL-2 under normal system condition (under three-phase fault on line 26–29)

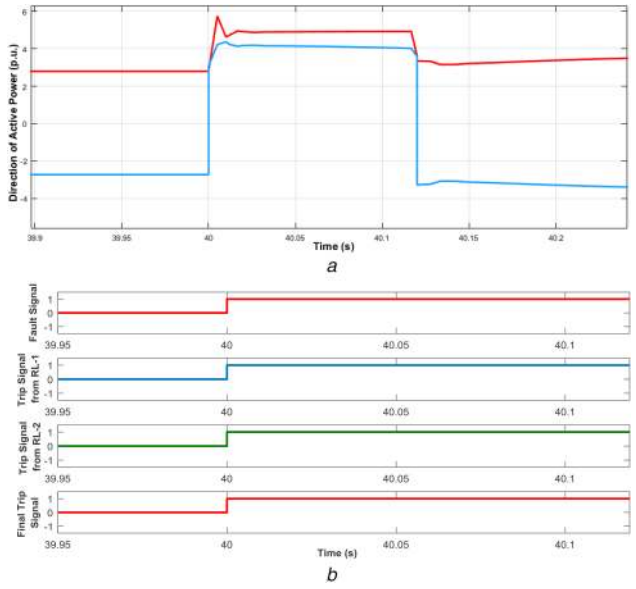

Fig. 7 *Performance of SABP scheme during high-impedance internal fault*
(a) DOAPF of RL-2 corresponding to line 26–29 under high-impedance three-phase fault on line 26–29, ***(b)*** Trip signals generated from RL-1 and RL-2 under high-impedance three-phase fault on line 26–29

3.2 Performance of SABP scheme under 'NORMAL' system state

Under normal operating conditions, the proposed SABP algorithm ensures a high degree of dependability aspect of distance relays as shown in Fig. 6*a*. This is validated for the relay corresponding to line 26–29 from bus 29 end. A three-phase fault (forward fault) with fault resistance of 10 Ω is incepted at 40 s on line 26–29 of the New England test system (Fig. 6*b*) and it is cleared at 40.12 s. Fig. 6*c* shows the fault inception signal; trip signals generated by RL-1 and RL-2; moreover, a final trip signal, which is produced due to the interaction of RL-1 and RL-2. The proposed scheme is validated on MATLAB 2015(b) environment using a desktop personal computer having Core-i7, 4 GHz processor, and 16 GB random access memory. This environment provides the response time of the proposed algorithm of the order of 1 cycle, i.e. it takes only 1 cycle to trigger the tripping signal by RL-1 and RL-2.

As a result, the final tripping signal is initiated exactly after 1 cycle of fault inception.

Table 1 Confusion matrix showing one misclassification of the event

Actual	Predicted			
	0	1	2	3
0	47	0	0	0
1	0	52	1	0
2	0	0	158	0
3	0	0	0	135

Table 2 Error matrix showing negligible error (in percentage)

Actual	Predicted				
	0	1	2	3	Error
0	0.12	0.00	0.0	0.00	0.00
1	0.00	013	0.0	0.00	0.02
2	0.00	0.00	0.4	0.00	0.00
3	0.00	0.00	0.0	0.35	0.00

3.3 Performance of SABP scheme during high-impedance internal fault

While validating any protection scheme, it is equally important for that scheme to detect high-impedance fault. For the same, a three-phase fault with fault resistance of 85 Ω is incepted on 50% of the line 26–29 at 40 s and cleared at 40.12 s. The assisting algorithm in place (RL-2) shows expected behaviour and maintains DOAPF from both the ends to be positive during faulty period. This can be seen in Fig. 7*a*. Thus, the final trip signal is generated due to the participation of both the RLs as shown in Fig. 7*b*.

3.4 Performance of SABP scheme during load encroachment

To validate the stable operation of the proposed algorithm for this situation, the test system is subjected to distributed load increment in order to bring load encroachment scenario. Owing to extreme loading condition, the impedance seen by the relay corresponding to line 26–29 (from bus 29 end) encroaches zone-3 as shown in Fig. 8*a*. As the apparent impedance enters the zone-3, RL-1 gets triggered. This is how the security aspect of existing CZBP scheme is compromised due to zone-3 mal-operation under load encroachment. However, RL-2, which utilises DOAPF information, has efficiently discriminated between the load encroachment and an internal fault on line 26–29 as shown in Fig. 8*b*. Therefore, even if RL-1 sends trip signal, due to the assistance provided by RL-2 in the proposed algorithm, final trip signal remains 0. This can be seen in Fig. 8*c*.

3.5 Performance of SABP scheme during stable power swing

To validate the performance of the proposed SABP algorithm, stable power swing situation is also simulated and tested. To obtain stable swing in line 26–29, a three-phase fault is incepted on line 28–29 at 12 s. Three-phase circuit breakers installed on line 28–29 are opened at 12.1 s to isolate the faulted element from rest of the system. Owing to sudden outage of line 28–29 post-three-phase fault, power swings through line 26–29. This is very well depicted in Fig. 9*a*, which illustrates how the apparent impedance passes into the ʊ circle of distance relay due to power swing. Fig. 9*b*

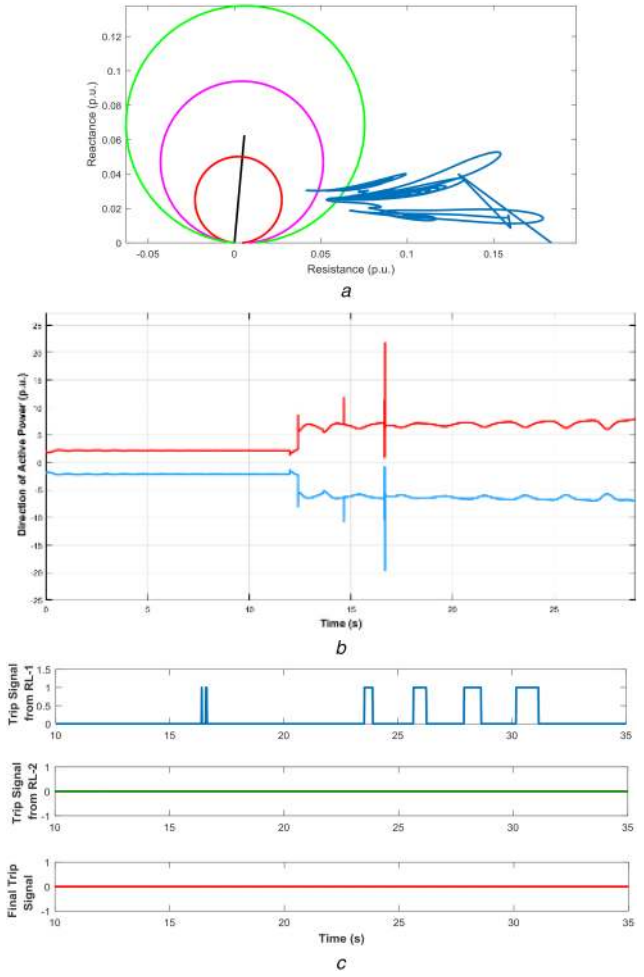

Fig. 8 *Performance of SABP scheme during load encroachment*
(a) Trajectory of apparent impedance during load encroachment, ***(b)*** DOAPF of RL-2 corresponding to line 26–29 during load encroachment, ***(c)***Trip signals generated from RL-1 and RL-2 during load encroachment

shows the expected performance of RL-2 algorithm under stable power swing through line 26–29 due to the outage of line 28–29. Fig. 9*c* shows the trip signals generated by RL-1, RL-2, and SABP scheme.

3.6 Response time and communication issues

The response time of any protection algorithm is defined as the time difference between the instant of fault inception and the instant of fault detection. This time includes pre-processing of raw input signals followed by phasor estimation, and finally calculations of steps included in the algorithm. To observe the response time of the proposed SABP algorithm, a three-phase fault is incepted at 50% of line 26–29 at 40 s (sample number 2657 of Fig. 6*c*). Following fault inception, the apparent impedance enters zone-1 of relay at bus 29 (Fig. 6*a*). Before entering zone-1, the AI crosses zone-3 (RL-1) of the same relay as evident from Fig. 6*a*. Fig. 6*c* shows the trip signals generated by both RL-1 and RL-2 following fault inception on line 26–29.

It is observed that both RL-1 (zone-1 and zone-2 are assumed to be non-operational in this particular test case) and RL-2 consume around 1 cycle to detect the fault following fault inception. As both the RLs are connected through logical AND operator, the final trip signal is generated exactly after 1 cycle of fault inception.

However, zone-3 (RL-1) generally operates with an intentional time delay of around 1–2 s [26]. Thus, even though RL-1 detects the fault within 1 cycle of fault inception, it still has to wait for around 1 s to generate its trip signal. This is illustrated in Fig. 10. When an intentional delay of 1 s is incorporated with RL-1, the trip signal is generated at 41 s. RL-2 works on wide-area information, which is inherently associated with communication latencies of the order of 100 ms [13, 18, 20]. Even though the response time of RL-2 is 1 cycle, however, if the latencies are considered while evaluating the response time, it is estimated to be around 100–200 ms as shown in Fig. 10. Owing to the considered latencies, the trip signal is generated at 40.1 s. Thus, an intentional delay is still required to be incorporated with RL-2 to have coordination with RL-1.

3.7 Comparative analysis with existing scheme

The existing BP logic employs the power swing blocking feature using concentric polygon blinder scheme. It is based on the fact that in case of a power swing, the apparent impedance reduces gradually and enters the third zone leading to miss-operation of the corresponding relay. On the occurrence of the symmetrical fault, the apparent impedance seen by the relay 'jumps' immediately to the fault impedance point. Therefore, in case of a stable power swing, the trajectory traverses the distance between the two blinders in more time as compared with the fault condition, where the trajectory of the apparent impedance will pass the blinder distance in no time.

The concurrent work is compared with the conventional blinder scheme for the relay corresponding to line 26–29 from bus 29 end. For the same, two concentric polygon blinder setting is done as per the standard guidelines [26]. The outer blinder (OB) is positioned with 20% security margin away from the maximum loadability on the resistive axis, inclined at the line impedance angle. Similarly, on the reactive axis, the OB setting is kept with 20% margin away from the third zone reach of the ʊ relay. Inner blinder (IB) is placed considering ΔZ to be around 10% of the OB [26].

The blinder setting details for the ʊ relay corresponding to line 26–29 from bus 29 end are shown below:

Resistive right OB (RROB): 0.0826 pu.
Resistive right IB (RRIB): 0.0743 pu.
Resistive left OB: −0.0826 pu.
Resistive left IB: −0.0743 pu.
The blinders are inclined at an angle of 84.79° as shown in Fig. 11*a*.
The reactive setting is done as shown below:
Reactive OB: 0.165 pu.
Reactive IB: 0.1485 pu.

The comparative analysis is discussed for different cases:

Case 1: Detection of stable power swing: Section 3.5 discusses the successful performance of SABP scheme when stable power swing has the tendency to initiate false tripping by the relay in consideration. To compare the performance of the existing blinder scheme and the proposed scheme, the stable swing is simulated by incepting an LLL-G fault on 50% of line 27–28 at 12 s. The line is opened at 12.4 s, which forces the power to swing through the adjacent line 26–29. Fig. 11*b* (which is the zoomed in version of Fig. 11*a*) shows that the impedance trajectory of the last cycle enters the RROB during a swing at 42.2759 s and after 148.6 ms touches the RRIB. Closer observation of *'trip signal from RL-1'* in Fig. 11*c* shows that it is the last swing cycle which enters zone-3 at 42.61 s (after it encroaches RRIB at 42.4245 s). This can be seen as an unstable power swing cycle by the employed blinder scheme. However, SABP scheme correctly identifies the stable condition, and thus it does not generate the final trip signal even when the last swing cycle enters zone-3. Fig. 11*c* shows the final relaying decision taken by SABP scheme. Similar observations are made in [27].

Case 2: Detection of fast power swing cycle: The employed blinder scheme might fail in case of high-frequency power swing cycles [28, 29]. Such conditions are detected when the system keeps on accelerating leading to high values of slip frequency of the order of 5 Hz, without producing any electrical centre on the line. Thus, on one hand where the traditional blinder scheme might lose the security aspect, SABP scheme performs securely in such system conditions.

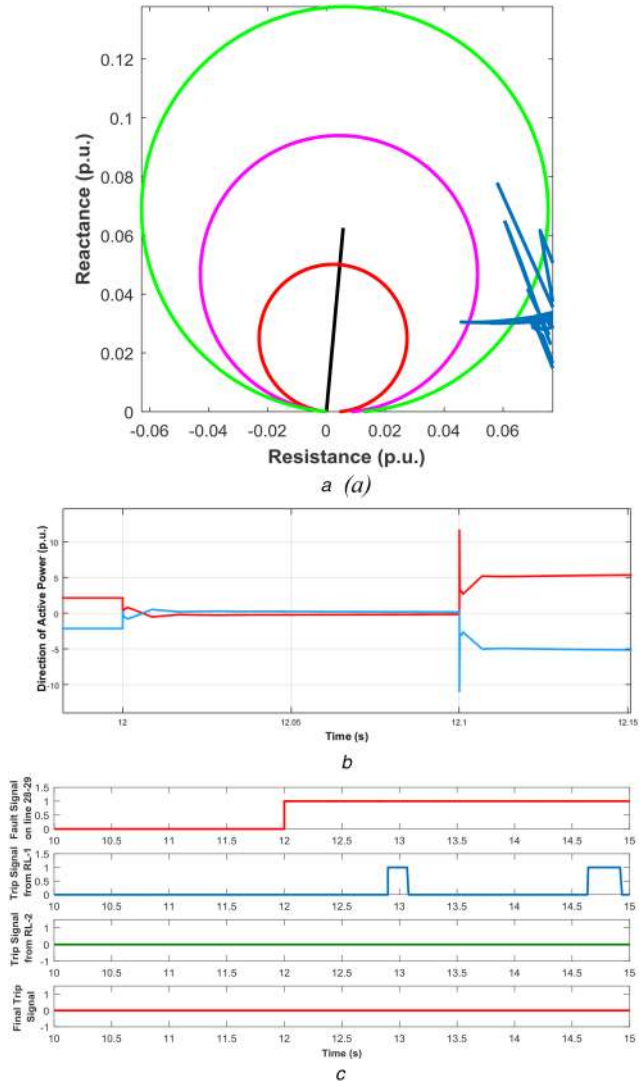

Fig. 9 *Performance of SABP scheme during stable power swing*
(a) Trajectory of apparent impedance during stable power swing, ***(b)*** DOAPF of RL-2 corresponding to line 26–29 during stable power swing, ***(c)*** Trip signals generated from RL-1 and RL-2 during a stable power swing

3.8 Salient features of the proposed scheme

Some of the salient features of the proposed SABP scheme are summarised below:

1. PMU information from only generator buses and boundary buses are used to assess the system state.
2. Less PMU information reduces the latencies involved in data propagation.
3. It works securely during stressed system condition.
4. Its dependability is maintained during forward faults.
5. Applicable for all types of shunt faults.

4 Conclusion

The research done through this work addresses the need of the development of an adaptable and more reliable protection scheme committed to protect the transmission lines. Training of the data-mining tool is done extensively. Huge dataset is generated to train DT by incepting all types of contingencies. Generation outages, line outages, and line faults are simulated at different locations of the test system to develop the required pool of data to train, validate, and test DT. The features to be fed into Rattle software are judiciously selected by locating the PMUs on critical buses. As a result, the performance of DT algorithm in yielding the system state is found to be encouraging. DOAPF algorithm as an assisting RL has also produced promising results during stressed system

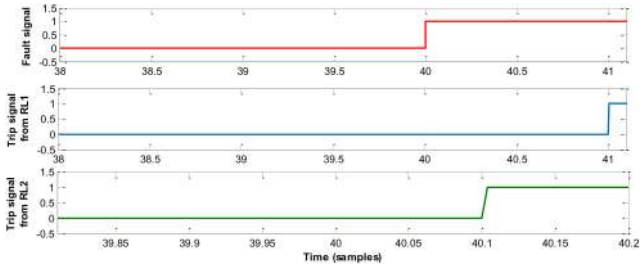

Fig. 10 *Trip signals generated by RL-1 and RL-2*

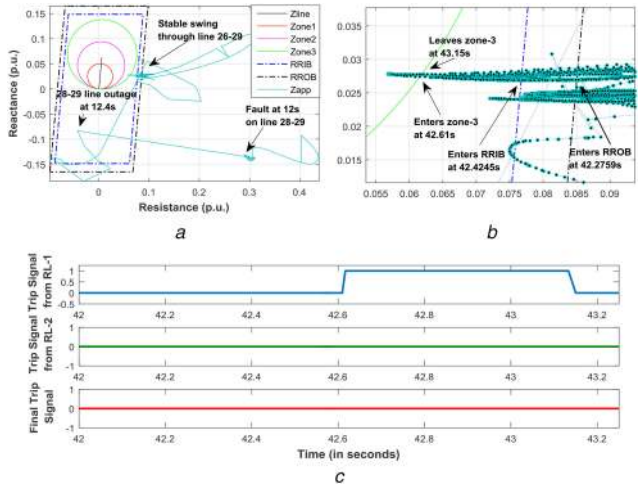

Fig. 11 *Comparative analysis with existing scheme*
(a) Blinder scheme wrongly identifies stable swing as out of step condition, ***(b)*** Zoomed in version of Fig. 11*a*, ***(c)*** Performance of SABP scheme during the stable swing

conditions. This RL accurately locates the faulted line, which is an essential development in assisting RL-1. The final trip signal which is generated due to the integration of RL-1 and RL-2 maintains dependability–security bias of the proposed protection logic. Unlike the traditional blinder scheme which has the tendency to compromise on the security trait of the protection logic under high-frequency swing, the proposed *SABP* scheme performs satisfactorily.

5 References

[1] Mason, C.R.: '*The art and science of protective relaying*' (Wiley, Hoboken, NJ, USA, 1956), ISBN 0471575526, 9780471575528

[2] North American Electric Reliability Council.: '*August 14, 2003 blackout: NERC actions to prevent and mitigate the impacts of future cascading blackouts*' (Princeton, NJ, USA, 2004)

[3] Report on the Grid Disturbance on 30th July 2012 and Grid Disturbance on 31st July 2012. Available at http://www.cercind.gov.in/2012/orders/Final_Report_Grid_Disturbance.pdf, accessed August 2012

[4] Blackout Report of Denmark. Available at http://www.geocities.jp/ps_dictionary/blackout/Final_report_uk-web.pdf, accessed September 2003

[5] Phadke, A.G., Thorp, J.S.: '*Synchronized phasor measurements and their applications*' (Springer, New York, USA, 2008)

[6] Terzija, V., Valverde, G., Cai, D., *et al.*: 'Wide-area monitoring, protection, and control of future electric power networks', *Proc. IEEE*, 2011, **99**, (1), pp. 80–93

[7] Phadke, A.G., Thorp, J.S.: 'Communication needs for wide area measurement applications'. Presented at the Fifth Critical Infrastructure Int. Conf., Beijing, China, September 2010

[8] Kamwa, I., Geoffroy, L., Samantaray, S.R., *et al.*: 'Synchrophasors data analytics framework for power grid control and dynamic stability monitoring', *IET Eng. Technol. Ref.*, DOI: 10.1049/etr.2015.0049

[9] Phadke, A., Well, P., Ding, L., *et al.*: 'Improving the performance of power system protection using wide area monitoring systems', *J. Mod. Power Syst. Clean Energy*, 2016, **4**, (3), pp. 319–331

[10] Horwitz, S.H., Phadke, A.G.: 'Third zone revisited', *IEEE Trans. Power Deliv.*, 2006, **21**, (1), pp. 23–29

[11] IEEE PSRC WG D6.: 'Power swing and out-of-step considerations on transmission lines', Final draft, June 2005

[12] Jin, M., Sidhu, T.S.: 'Adaptive load encroachment prevention scheme for distance protection', *Electr. Power Syst. Res.*, 2008, **78**, pp. 1693–1700

[13] Eissa, M.M., Masoud, M.E., Elanwar, M.M.M.: 'A novel back-up wide area protection technique for power transmission grids using phasor measurement unit', *IEEE Trans. Power Deliv.*, 2010, **25**, (1), pp. 270–278

[14] Bernabeu, E.E., Thorp, J.S., Centeno, V.: 'Methodology for a security/dependability adaptive protection scheme based on data mining', *IEEE Trans. Power Deliv.*, 2012, **27**, (1), pp. 104–111
[15] Jena, M.K., Samantaray, S., Panigrahi, B.: 'A new adaptive dependability–security approach to enhance wide area back-up protection of transmission system', *IEEE Trans. Smart Grid*, 2017, **PP**, (99), pp. 1–1, doi: 10.1109/TSG.2017.2710134
[16] Nayak, P.K., Pradhan, A.K., Bajpai, P.: 'Wide-area measurement-based backup protection for power network with series compensation', *IEEE Trans. Power Deliv.*, 2014, **29**, (4), pp. 1970–1977
[17] Zare, J., Aminifar, F., Sanaye-Pasand, M.: 'Synchrophasor-based wide-area back-up protection scheme with data requirement analysis', *IEEE Trans. Power Deliv.*, 2015, **30**, (3), pp. 1410–1419
[18] Jena, M.K., Samantaray, S.R., Panigrahi, B.K.: 'A new wide-area backup protection scheme for series-compensated transmission system', *IEEE Syst. J.*, 2017, **11**, (3), pp. 1877–1887
[19] Dubey, R., Samantaray, S.R., Panigrahi, B.K.*, et al.*: 'Koopman analysis based wide-area back-up protection and faulted line identification for series-compensated power network', *IEEE Syst. J.*, 2016, **PP**, (99), pp. 1–11
[20] Jena, M.K., Samantaray, S.R., Panigrahi, B.K.: 'A new decentralized approach to wide-area back-up protection of transmission lines', *IEEE Syst. J.*, 2017, **PP**, (99), pp. 1–8, DOI: 10.1109/JSYST.2017.2694453
[21] Supreme, H., Dessaint, L.A., Kamwa, I.*, et al.*: 'Development of new predictors based on the concept of center of power for transient and dynamic instability detection', *IEEE Trans. Smart Grid*, 2016, **PP**, (99), pp. 1–1, DOI: 10.1109/TSG.2016.2636816
[22] Kamwa, I., Pradhan, A.K., Joos, G.*, et al.*: 'Fuzzy partitioning of a real power system for dynamic vulnerability assessment', *IEEE Trans. Power Syst.*, 2009, **24**, pp. 1356–1365
[23] Chow, H.: '*Power system coherency and model reduction*' (Springer, New York, NY, USA, 2013)
[24] Eissa, M.M.: 'Development and investigation of a new high-speed directional relay using field data', *IEEE Trans. Power Deliv.*, 2008, **23**, (3), pp. 1302–1309
[25] Eissa, M.M.: 'A new digital feed circuit protection using directional element', *IEEE Trans. Power Deliv.*, 2009, **24**, (2), pp. 531–537
[26] Ziegler, G.: '*Numerical distance protection principles and application*' (Siemens-Erlangen Publicis, Germany, 1999)
[27] Kang, D., Gokaraju, R.: 'A new method for blocking third-zone distance relays during stable power swings', *IEEE Trans. Power Deliv.*, 2016, **31**, (4), pp. 1836–1843
[28] Lavand, S.A., Soman, S.A.: 'Predictive analytic to supervise zone 1 of distance relay using synchrophasors', *IEEE Trans. Power Deliv.*, 2016, **31**, (4), pp. 1844–1854
[29] Mooney, J., Fischer, N.: 'Application guidelines for power swing detection on transmission systems'. Proc. 59th Annual Conf. Protection Relay Engineering, College Station, TX, USA, 2006, p. 10